Supplementary Material (ESI) for Chemical Communications

Supporting Information for:

Solid-State Materials for Anion Sensing in Aqueous Solution: Highly Selective Colorimetric and Luminescence-Based Detection of Perchlorate Using a Platinum(II) Salt

Stephen D. Taylor,[†] Whitney Howard,[†] Necati Kaval,[†] Robert T. Hart,[‡] Jeanette A. Krause,[†] and William B. Connick[†,*]
Department of Chemistry, University of Cincinnati, P.O. Box 210172, Cincinnati, Ohio 45221-0172 and The Shepherd Chemical Company, 4900 Beech St., Norwood, Ohio 45212.

Experimental Section:

K_2PtCl_4 was purchased from Pressure Chemical. COD (1,5-cyclooctadiene) and tpy (2,2′:6′2″-terpyridine) were obtained from Aldrich. NH_4PF_6 was purchased from Alfa Aesar. NH_4ClO_4, $NaClO_4$, $NaSO_4$, NaCl, $NaHCO_3$, $NaNO_3$, $NaClO_4$, and Na_3PO_4 were purchased from Fischer Scientific. Starting materials, $Pt(COD)Cl_2$ and $[Pt(tpy)Cl]Cl•2H_2O$, were prepared according to published procedures.[1,2] HYPAN80 was purchased from Hymedix International. Vycor porous glass rods (4"x 0.112") were purchased from Advanced Glass and Ceramics and cut to into 0.125" long segments. Ohio River water was sampled at Sawyer Point in Cincinnati, OH.

$Pt(tpy)Cl^+$ salts were prepared by a modification of a published procedure.[3] Yellow needles of $[Pt(tpy)Cl]PF_6$ (**1**•PF_6) were grown from acetone/water. Anal Calcd for $C_{15}H_{11}N_3ClF_6PPt$ (FW: 608.99): C, 29.60; H, 1.82; N, 6.90. Found: C, 29.70; H, 1.75; N, 6.91. MS-ESI (positive ion mode, CH_3CN) (m/z): 464.0 ($Pt(tpy)Cl^+$). MS-ESI (negative ion mode, CH_3CN) (m/z): 144.9 (PF_6^-). Red needles of $[Pt(tpy)Cl]ClO_4.H_2O$ (**1**•$ClO_4.H_2O$) were grown from acetone/water. Anal Calcd for $C_{15}H_{11}N_3Cl_2O_4Pt.H_2O$ (FW:581.27): C, 30.00; H, 2.25; N, 7.23. Found: C, 31.23; H, 1.92; N, 7.12. MS-ESI (positive ion mode, MeCN) (m/z): 464.0. MS-ESI (negative ion mode, MeCN) (m/z): 100.9.

Preparation of HYPAN80 and Vycor Supported Materials. HYPAN80 membranes were prepared from a solution of 10% HYPAN80 (w/w) in DMSO. The mixture was stirred and heated at ~80 ^{o}C overnight to give a colorless viscous solution. Two pieces of Teflon tape were placed on the long sides of a microscope slide, resulting in an approximately 101 mm x 13 mm x 76 μm (length x width x thickness) area into which the HYPAN80 solution was poured. The membrane was hardened by soaking in water and subsequently washed well with water to give a colorless transparent membrane. The polymer membrane was stored in water in between uses. Colored HYPAN80 membranes containing the platinum complexes were prepared in a similar fashion, adding 10 mg of **1**•PF_6 (or **1**•$ClO_4.H_2O$) per g of 10% HYPAN80/DMSO solution.

Pieces of **1**•PF_6 (or **1**•$ClO_4.H_2O$) supported Vycor porous glass were prepared by immersing dried porous glass pieces in a 0.75% w/w solution of **1**•PF_6 and 50% v/v DMSO/acetone solution for several hours. The resulting yellow pieces of glass were submerged in water to induce precipitation of the complex within the glass matrix. The samples were allowed to air dry for 1 hour, before drying under vacuum at 90°C overnight to give translucent yellow/orange pieces of Vycor porous glass. Dried pieces of porous glass were stored in a closed vial until use. The yellow color of both the polymer membranes and pieces of Vycor porous fades overtime. Additionally, small colored particulates start to collect on the bottom of the vials of water in which the polymer membranes were stored, which is consistent with leaching out.

Characterization. Elemental analyses were performed by Atlantic Microlab (Norcross, GA). A sample of **1**•PF_6 was ground with a mortar and pestle, immersed in 1 M NH_4ClO_4 for

~18 hr, and washed with copious amounts of water. The analysis results are consistent with exchange of ~55% of the PF_6^- for ClO_4^- and H_2O. Anal Calcd for $C_{15}H_{12.1}N_3Cl_{1.55}F_{2.7}O_{2.75}P_{0.45}Pt$: C: 30.35; H: 2.05; O: 7.41; Cl: 9.26; F: 8.64. Found: C: 30.85; H: 1.73; O: 6.78; Cl: 9.79; F: 8.05. Mass spectra were obtained using a Micromass Q- Tof 2 (Waters, Milford, MA, USA). The instrument conditions were optimized and calibrated in positive ion mode using poly-alanine (Sigma, St. Louis, MO, USA) and in negative ion mode using sodium iodide (Fisher Scientific). The observed isotope patterns agreed well with those predicted based on natural isotopic abundances. Laser desorption ionization mass spectra were obtained using a Bruker BIFLEX III (Billerica, MA, USA) with a nitrogen laser. A powder sample of **1**•PF_6 was immersed in aqueous 1 M NH_4ClO_4, washed with copious amounts of water and dried. The powder was pressed with a spatula onto a laser desorption plate. The instrument was externally calibrated using two peptide standards: bradykinin (frag. 1-5), 573.31 Da and adrenocorticotropic hormone (frag. 18-39), 2465.19 Da (Sigma, St. Louis, MO, USA). Mass spectra are the result of an average of 200 to 400 single laser shot mass spectra.

UV-visible absorption spectra were recorded using a Varian Cary 50Bio UV-visible absorption spectrophotometer. To monitor the absorption spectra of **1**•PF_6 and **1**•$ClO_4.H_2O$ in HYPAN80 membranes, a ~10 x 10 mm section of membrane was fixed inside a standard 1 cm pathlength quartz cuvette. A baseline spectrum was determined using a HYPAN80 membrane without the platinum complex in water. To monitor the absorption spectra of **1**•PF_6 exposed to 0.1 M ClO_4^-, the **1**•PF_6 HYPAN80 film was fixed inside a cuvette and 0.1 M NH_4ClO_4 was added slowly over a period of ~15 s. Spectra in Figure 2A were collected after addition was complete. Solubilities were estimated using a HP8453 diode array spectrometer to determine the $Pt(tpy)Cl^+$ concentrations (330 nm, 21,600 $M^{-1}cm^{-1}$; and 250 nm, 44,400 $M^{-1}cm^{-1}$) of saturated aqueous solutions of **1**•$ClO_4.H_2O$ and **1**•PF_6 obtained by heating a mixture of the given salt in water and allowing the mixture to stand at room temperature (23 °C) for 24 hours. Obtained solutions were filtered and then diluted prior to concentration measurements in order to avoid aggregation effects. Values for 5 solutions of each salt were averaged to obtain estimates of K_{sp} (**1**•PF_6, $9.5(6) \times 10^{-10}$ M^2; **1**•$ClO_4.H_2O$, $9.4(3) \times 10^{-9}$ M^2).

Emission samples were excited using a 532 nm solid-state laser (Melles Griot, Carlsbad CA). Laser power was reduced to 0.1 mW using a neutral density filter. Emissions were detected using a bifurcated 6:1 fiber optic bundle and transferred to an Acton SpectraPro 300i spectrophotometer equipped with a photon counter PMT detector. A holographic notch filter from Kaiser Optical Systems, Inc. was placed at the entrance slit of the spectrophotometer to filter the 532 nm laser beam. For emission measurements using the platinum complex supported on porous glass, a piece of the porous glass was placed at the tip of a short piece of teflon tubing attached to the fiber optic bundle. The porous glass was dipped in aqueous solution to give a real-time emission response to perchlorate. Corrected steady-state emission data were collected using a SPEX Fluorolog-3 fluorimeter equipped with a double emission monochromator and a single excitation monochromator. Uncorrected emission spectra obtained for powder samples of **1**•$ClO_4.H_2O$ using the 532 nm solid-state laser exhibits a maximum at 670 nm; the corrected maximum is 690 nm. ATR-IR spectra were obtained using a Nicolet 6700 FTIR with a Smart Orbit diamond crystal ATR attachment from Thermo Fisher Scientific.

Scanning electron microscopy and energy dispersive X-ray spectroscopy (SEM-EDS) measurements were carried out using a FEI XL-30 scanning electron microscope. Secondary-emission electron images were collected using 15 kV accelerating potential and a 5.6 µm spot size with 80× magnification. X-ray spectra were collected from 0.10 to 20.58 keV in 2048 channels for 30 s using a liquid N_2 cooled Si(Li) detector. Count rates were typically ~4000 s^{-1}. For elemental analysis and mapping, windows were identified near the following peaks: $O_{K\alpha}$ (0.42-0.58 keV), $F_{K\alpha}$ (0.62-0.74 keV), $P_{K\alpha 1}/Pt_{M\alpha 1+M\beta}$ (1.93-2.25 keV) and $Cl_{K\alpha 1}$ (2.51-2.73 keV). Since the peaks for P and Pt overlap, the map for that window represents both elements. The EDS images were collected in 100×128 points with a count time of 1.0 s per point. The saturations of the pixel colors for the false-color image in Figure 3 are proportional to the number of counts, with the maximum number of counts per map being set to full saturation.

X-ray Crystallography. For X-ray examination and data collection, suitable single crystals, approximate dimensions 0.11 × 0.02 × 0.01 mm (**1**•PF_6) and 0.18 × 0.03 × 0.02 mm (**1**•$ClO_4.H_2O$), were mounted in a loop with paratone-N and transferred immediately to the goniostat bathed in a cold stream.

Intensity data were collected at 150K using a Bruker SMART6000 CCD diffractometer with graphite-monochromated Cu Kα radiation, λ=1.54178Å. Data collection frames were measured at 0.3° intervals of ω with a maximum 2θ value of ~135° and processed using the program SAINT. The data were corrected for decay, Lorentz and polarization effects as well as absorption and beam corrections based on the multi-scan technique as implemented in SADABS.[4]

The structures were solved by a combination of direct methods and the difference Fourier technique using SHELXTL and refined by full-matrix least squares on F^2. Non-hydrogen atoms were refined with anisotropic displacement parameters with the exception of the minor component of the disordered F atoms for **1**•PF_6. The hydrogen atoms on the cation were calculated and treated with a riding model. The water hydrogen atoms were located directly from the difference map; the positions were then held at this location in subsequent refinements. The isotropic displacement parameters for the H-atoms were defined as a*U_{eq} of the adjacent atom, (a=1.5 for O-H and 1.2 for all others). The PF_6^- counterion in **1**•PF_6 shows typical disorder; this was addressed with a two-component model (78-86% occupancy range for the major component). The refinement converged with crystallographic agreement factors as summarized in Table S1. The ORTEP drawings of **1**•PF_6 and **1**•$ClO_4.H_2O$ are shown in Figure S6. A complete listing of bond distances and angles are given in Table S2. All additional crystallographic details can be obtained from the CIF.

X-Ray Powder Diffraction. Data for **1**•PF_6 were collected at the Advanced Photon Source station 11-BM, Argonne National Laboratory using 0.458884 Å photons in transmission geometry as the sample was rotated. The incident photons were selected with platinum striped mirrors and a double Si(111) monochromator with adjustable sagittal focus. The scattered beams were selected with (12) perfect Si(111) analyzer crystals. Discrete detectors covering an angular range from -6 to 16° 2θ were scanned over a 34° 2θ range, with data points collected every 0.001° 2θ and scan speed of 0.01°/s. Complete descriptions of the instrument and data collection system have been reported previously.[5-7]

For **1**•$ClO_4.H_2O$ and **1**•PF_6 exposed to ClO_4^-, the data were collected on a Rigaku D-max 2100 diffractometer in Bragg-Brentano θ-2θ geometry (Cu K_α; scintillation detector; $5 \leq 2\theta \leq 60°$ [**1**•$ClO_4.H_2O$]; $5.00 \leq 2\theta \leq 44.28°$ [**1**•PF_6 exposed to ClO_4^-]; step size = 0.02°; data collection time = 4 s/point). For **1**•$ClO_4.H_2O$, a curved graphite (002) analyzer crystal was used on the diffracted beam. Both samples were exposed to water-vapor saturated air immediately prior to data collection.

Simulated powder diffraction patterns were calculated from the corresponding single-crystal structures using the program Mercury 1.4.2 (available for download from the CCDC).

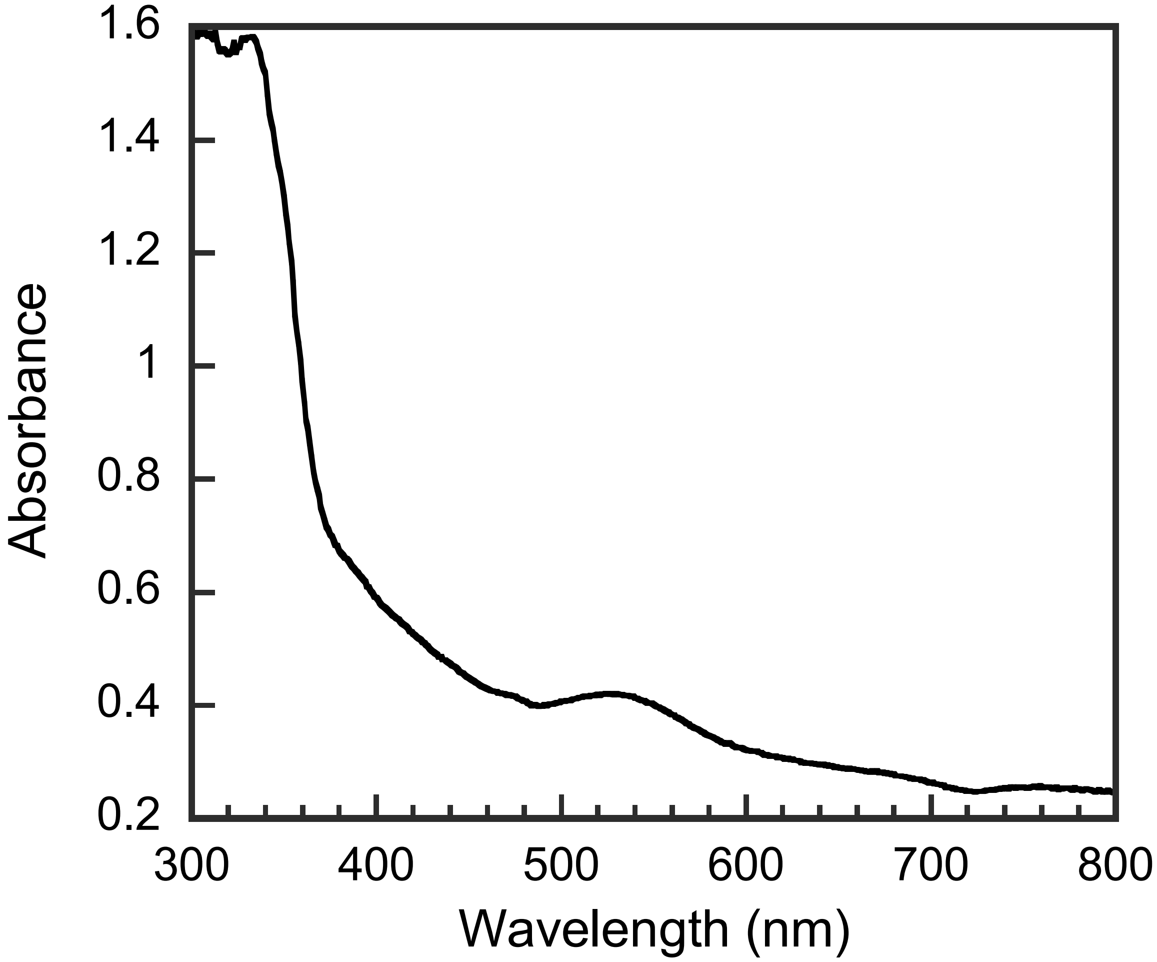

Figure S1: UV-visible absorption spectrum of **1**•$ClO_4.H_2O$ supported in a HYPAN80 film.

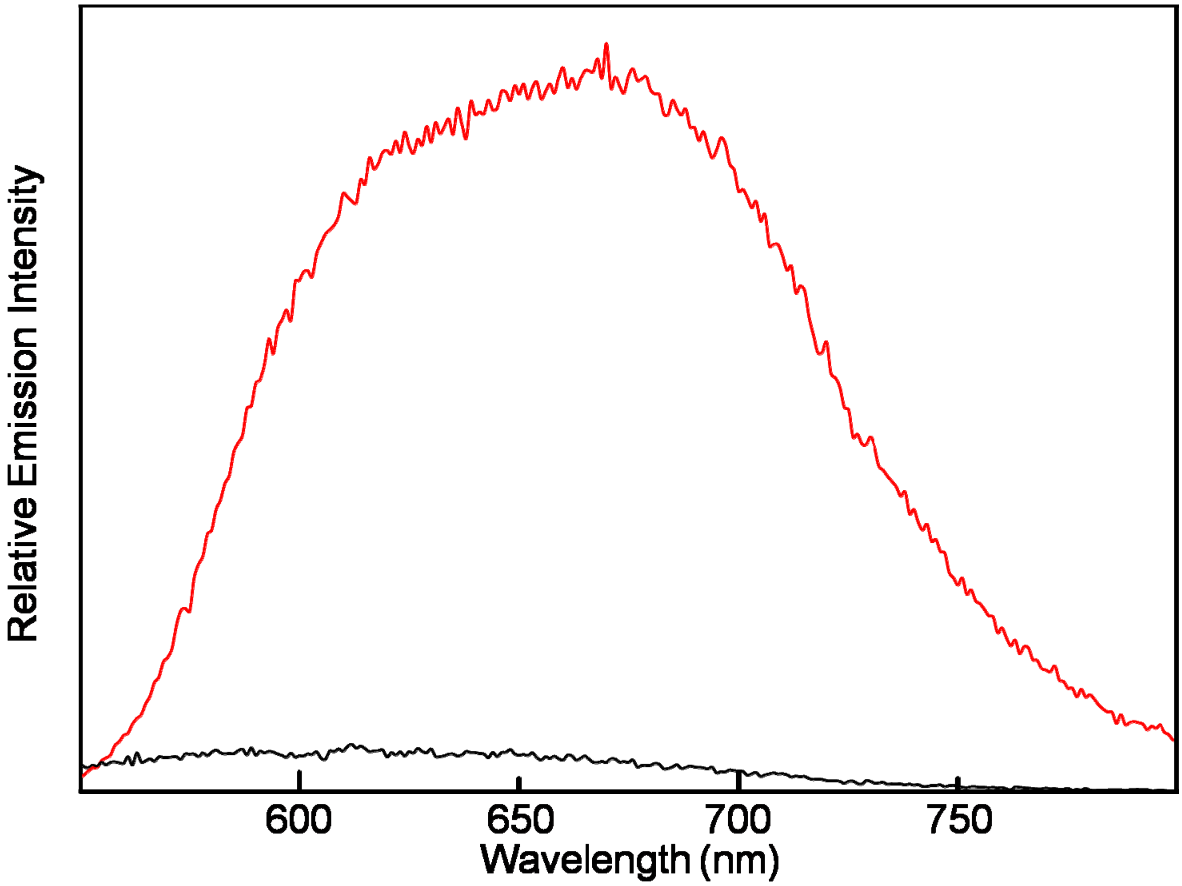

Figure S2. Uncorrected emission spectra of Vycor porous glass supported **1**•PF_6 (—) and **1**•$ClO_4.H_2O$ (—) in water (λ_{ex} = 532 nm).

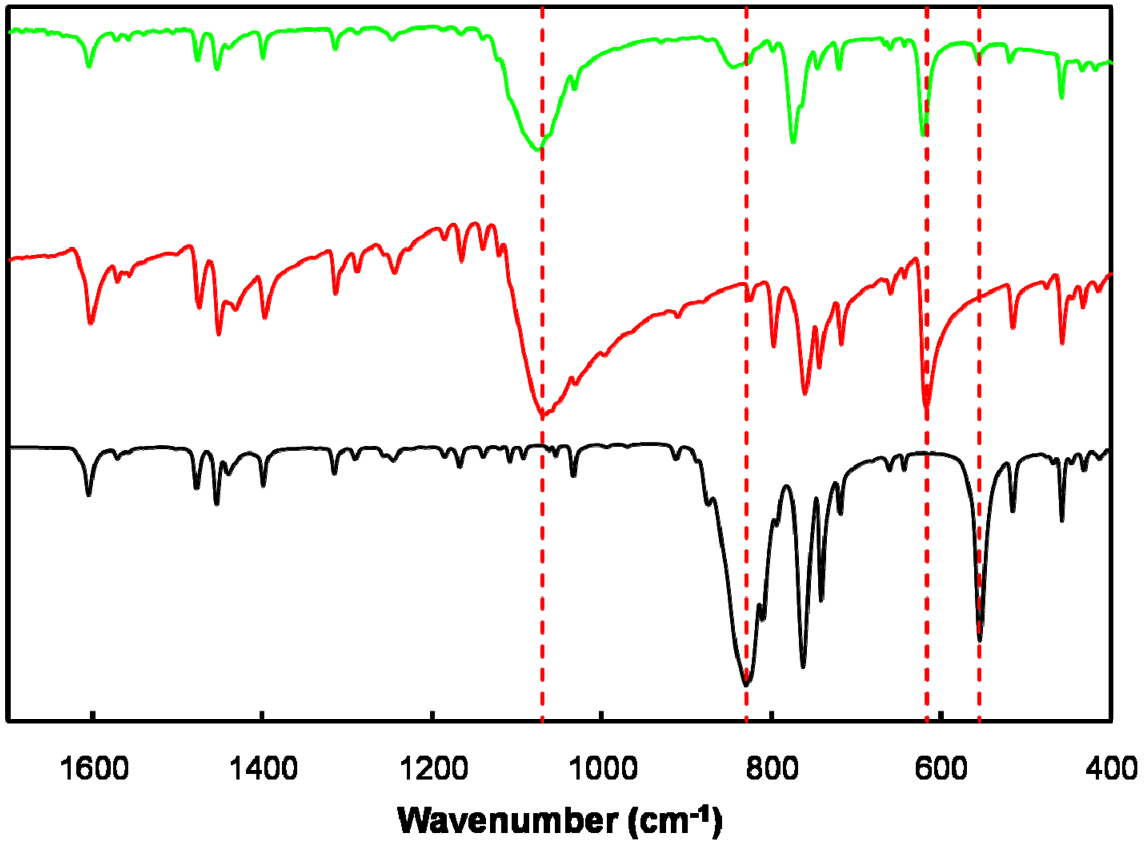

Figure S3. ATR-IR spectra of **1**•PF_6 (—), **1**•ClO_4 (—) and **1**•PF_6 after exposure to 1.0 M NH_4ClO_4 (—). Red vertical lines indicate signature bands for ClO_4^- and PF_6^-.

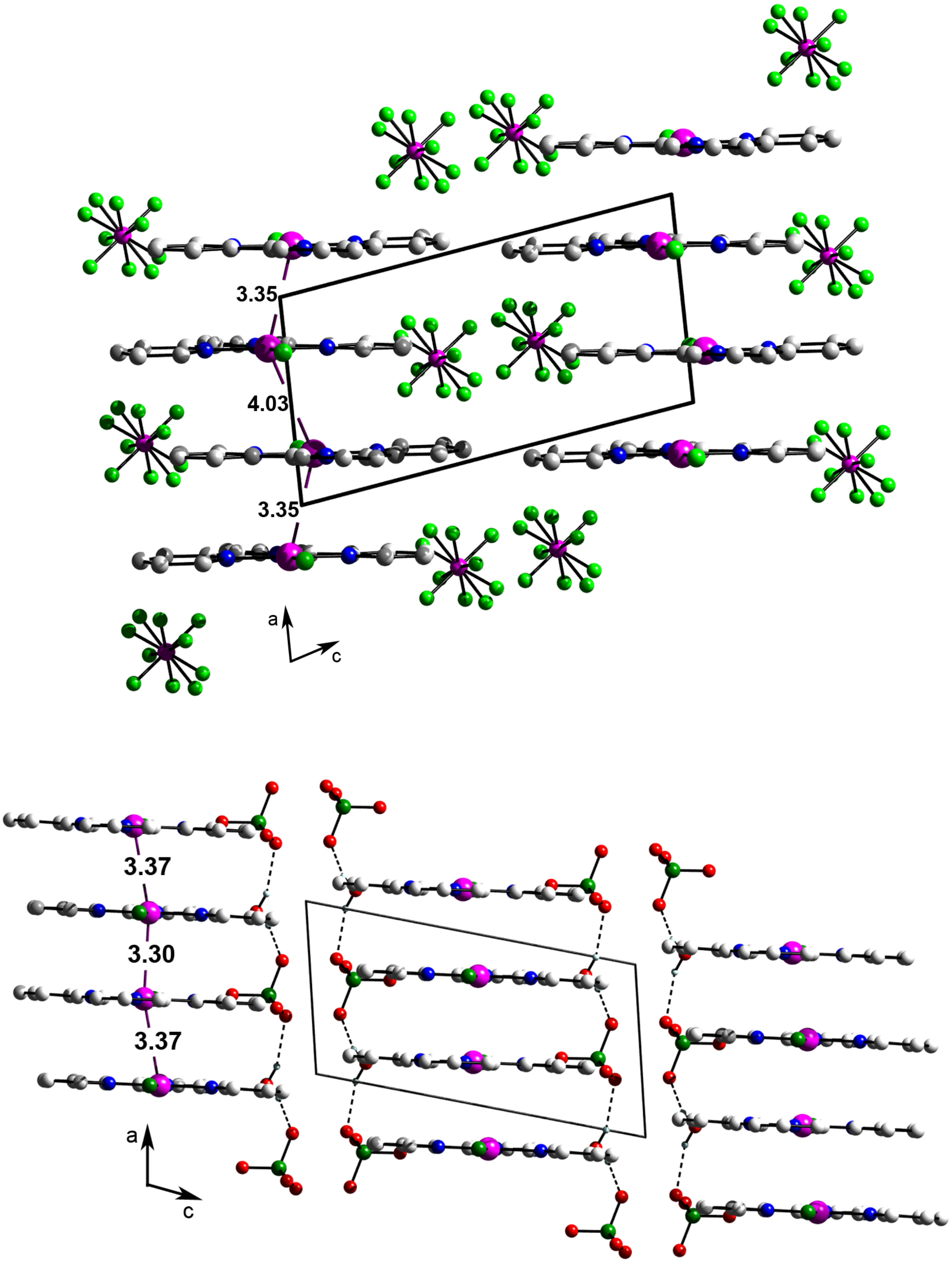

Figure S4. Crystal packing for **1**•PF_6 (top) and **1**•$ClO_4.H_2O$ (bottom) viewed down the *b* axes. H-atoms are omitted for clarity.

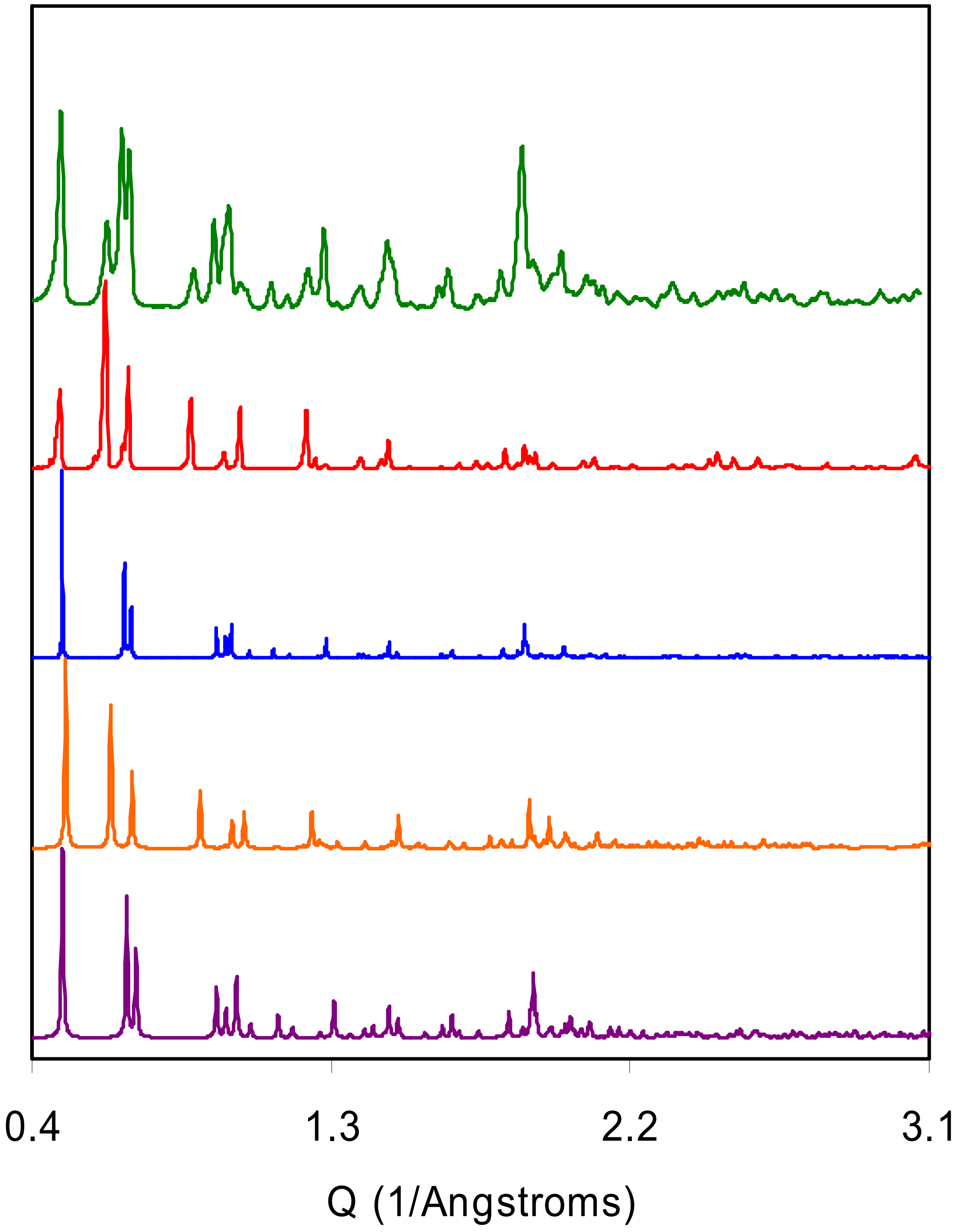

Figure S5. X-ray powder diffractograms of **1**•PF_6 exposed to 1 M NH_4ClO_4 for 24 hours (—), **1**•$ClO_4.H_2O$ (—) and **1**•PF_6 (—). Simulated powder diffraction patterns for **1**•$ClO_4.H_2O$ (—) and **1**•PF_6 (—).

Table S1. Single Crystal X-ray Data Summary.

	1•PF_6	**1•$ClO_4.H_2O$**
Formula	$[C_{15}H_{11}N_3ClPt]PF_6$	$[C_{15}H_{11}N_3ClPt]ClO_4.H_2O$
Formula weight	608.78	581.27
Temperature, K	150(2)	150(2)
Wavelength, Å	1.54178	1.54178
Crystal system	Triclinic	Triclinic
Space group	P-1	P-1
Unit cell dimensions:	a = 6.8718(1) Å	a = 6.6281(2) Å
	b = 9.9804(2) Å	b = 10.2133(3) Å
	c = 13.7574(2) Å	c = 13.3506(4) Å
	α = 69.993(1)°	α = 104.376(1)°
	β = 76.976(1)°	β = 103.628(1)°
	γ = 74.599(1)°	γ = 90.548(2)°
Volume	845.28(2) $Å^3$	848.59(4) $Å^3$
Z	2	2
Density (calculated), Mg/m^3	2.392	2.275
Absorption coefficient, mm^{-1}	18.546	18.684
F(000)	572	552
Crystal size, mm^3	0.11 x 0.02 x 0.01	0.18 x 0.03 x 0.02
θ range for data collection	3.46 to 67.54°	3.53 to 67.47°
Index ranges	$-8 \le h \le 8$	$-7 \le h \le 7$
	$-11 \le k \le 11$	$-12 \le k \le 11$
	$-16 \le l \le 16$	$-15 \le l \le 15$
Reflections collected	6957	6610
Independent reflections	2870 [R_{int} = 0.0272]	2853 [R_{int} = 0.0335]
Completeness to θ = 67.47°	93.9 %	93.5 %
Absorption correction	Multi-scan	Multi-scan
Max. and min. transmission	0.8363 and 0.23480.	0.6963 and 0.5339
Refinement method	Full-matrix least-squares on F^2	
Data / restraints / parameters	2870 / 0 / 260	2853 / 0 / 235
Goodness-of-fit on F^2	1.056	1.011
Final R indices [I>2σ(I)]	R1 = 0.0240	R1 = 0.0348
	wR2 = 0.0604	wR2 = 0.0821
R indices (all data)	R1 = 0.0267	R1 = 0.0401
	wR2 = 0.0618	wR2 = 0.0843
Largest diff. peak and hole	1.134 and -0.792 $eÅ^{-3}$	1.939 and -1.109 $eÅ^{-3}$

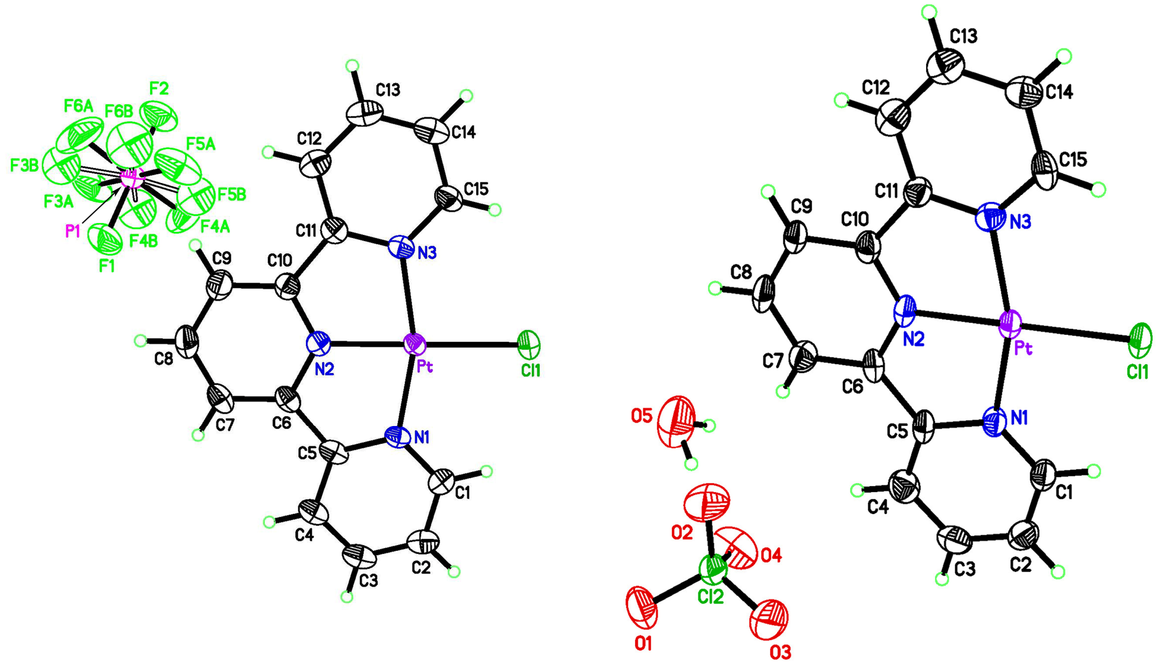

Figure S6. ORTEP diagrams for **1**•PF_6 (left) and **1**•$ClO_4.H_2O$ (right) showing 50% probability thermal ellipsoids and atomic labeling scheme.

Table S2. Bond Distances (Å) and Angles (°) from Single Crystal X-ray Data.

1•PF$_6$		**1•ClO$_4$.H$_2$O**	
Pt-N(2)	1.949(4)	Pt-N(2)	1.943(5)
Pt-N(1)	2.016(4)	Pt-N(1)	2.031(5)
Pt-N(3)	2.023(4)	Pt-N(3)	2.043(5)
Pt-Cl(1)	2.3058(10)	Pt-Cl(1)	2.3101(15)
N(1)-C(1)	1.346(6)	N(1)-C(1)	1.336(9)
N(1)-C(5)	1.357(6)	N(1)-C(5)	1.387(8)
N(2)-C(6)	1.349(6)	N(2)-C(6)	1.347(9)
N(2)-C(10)	1.350(6)	N(2)-C(10)	1.349(9)
N(3)-C(15)	1.346(6)	N(3)-C(11)	1.337(9)
N(3)-C(11)	1.381(6)	N(3)-C(15)	1.353(9)
C(1)-C(2)	1.386(7)	C(1)-C(2)	1.380(11)
C(2)-C(3)	1.371(8)	C(2)-C(3)	1.369(11)
C(3)-C(4)	1.387(8)	C(3)-C(4)	1.388(11)
C(4)-C(5)	1.384(7)	C(4)-C(5)	1.385(11)
C(5)-C(6)	1.489(7)	C(5)-C(6)	1.464(10)
C(6)-C(7)	1.386(7)	C(6)-C(7)	1.383(10)
C(7)-C(8)	1.383(8)	C(7)-C(8)	1.393(11)
C(8)-C(9)	1.389(8)	C(8)-C(9)	1.402(10)
C(9)-C(10)	1.365(7)	C(9)-C(10)	1.374(10)
C(10)-C(11)	1.479(7)	C(10)-C(11)	1.489(9)
C(11)-C(12)	1.383(7)	C(11)-C(12)	1.387(10)
C(12)-C(13)	1.377(8)	C(12)-C(13)	1.380(11)
C(13)-C(14)	1.365(8)	C(13)-C(14)	1.385(11)
C(14)-C(15)	1.384(7)	C(14)-C(15)	1.388(11)
P(1)-F(6B)	1.45(4)	Cl(2)-O(3)	1.413(6)
P(1)-F(4B)	1.50(4)	Cl(2)-O(2)	1.423(6)
P(1)-F(5B)	1.50(2)	Cl(2)-O(4)	1.430(7)
P(1)-F(4A)	1.570(5)	Cl(2)-O(1)	1.435(6)
P(1)-F(6A)	1.572(5)		
P(1)-F(1)	1.582(4)		
P(1)-F(5A)	1.591(5)		
P(1)-F(3A)	1.592(5)		
P(1)-F(3B)	1.59(3)		
P(1)-F(2)	1.599(4)		
N(2)-Pt-N(1)	81.28(16)	N(2)-Pt-N(1)	81.3(2)
N(2)-Pt-N(3)	81.23(16)	N(2)-Pt-N(3)	80.6(2)
N(1)-Pt-N(3)	162.46(16)	N(1)-Pt-N(3)	162.0(2)
N(2)-Pt-Cl(1)	179.17(11)	N(2)-Pt-Cl(1)	179.74(17)
N(1)-Pt-Cl(1)	98.77(11)	N(1)-Pt-Cl(1)	98.73(16)
N(3)-Pt-Cl(1)	98.70(11)	N(3)-Pt-Cl(1)	99.32(17)
C(1)-N(1)-C(5)	118.7(4)	C(1)-N(1)-C(5)	119.5(6)

C(1)-N(1)-Pt	127.7(3)	C(1)-N(1)-Pt	128.5(5)
C(5)-N(1)-Pt	113.5(3)	C(5)-N(1)-Pt	112.1(4)
C(6)-N(2)-C(10)	124.6(4)	C(6)-N(2)-C(10)	123.8(6)
C(6)-N(2)-Pt	117.5(3)	C(6)-N(2)-Pt	118.0(5)
C(10)-N(2)-Pt	117.9(3)	C(10)-N(2)-Pt	118.2(5)
C(15)-N(3)-C(11)	119.5(4)	C(11)-N(3)-C(15)	121.0(6)
C(15)-N(3)-Pt	127.5(3)	C(11)-N(3)-Pt	113.2(4)
C(11)-N(3)-Pt	113.0(3)	C(15)-N(3)-Pt	125.8(5)
N(1)-C(1)-C(2)	121.7(5)	N(1)-C(1)-C(2)	121.7(7)
C(3)-C(2)-C(1)	119.1(5)	C(3)-C(2)-C(1)	119.7(7)
C(2)-C(3)-C(4)	120.2(5)	C(2)-C(3)-C(4)	119.7(7)
C(5)-C(4)-C(3)	118.0(5)	C(5)-C(4)-C(3)	119.2(7)
N(1)-C(5)-C(4)	122.2(5)	C(4)-C(5)-N(1)	120.2(7)
N(1)-C(5)-C(6)	115.0(4)	C(4)-C(5)-C(6)	124.2(6)
C(4)-C(5)-C(6)	122.7(5)	N(1)-C(5)-C(6)	115.5(6)
N(2)-C(6)-C(7)	118.0(4)	N(2)-C(6)-C(7)	118.8(7)
N(2)-C(6)-C(5)	112.6(4)	N(2)-C(6)-C(5)	113.1(6)
C(7)-C(6)-C(5)	129.4(4)	C(7)-C(6)-C(5)	128.0(7)
C(8)-C(7)-C(6)	118.7(5)	C(6)-C(7)-C(8)	118.9(7)
C(7)-C(8)-C(9)	121.2(5)	C(7)-C(8)-C(9)	120.4(7)
C(10)-C(9)-C(8)	119.0(5)	C(10)-C(9)-C(8)	118.6(7)
N(2)-C(10)-C(9)	118.5(5)	N(2)-C(10)-C(9)	119.4(6)
N(2)-C(10)-C(11)	112.9(4)	N(2)-C(10)-C(11)	112.1(6)
C(9)-C(10)-C(11)	128.6(5)	C(9)-C(10)-C(11)	128.4(7)
N(3)-C(11)-C(12)	120.4(5)	N(3)-C(11)-C(12)	121.0(7)
N(3)-C(11)-C(10)	114.9(4)	N(3)-C(11)-C(10)	115.8(6)
C(12)-C(11)-C(10)	124.6(5)	C(12)-C(11)-C(10)	123.2(7)
C(13)-C(12)-C(11)	119.4(5)	C(13)-C(12)-C(11)	118.9(8)
C(14)-C(13)-C(12)	119.7(5)	C(12)-C(13)-C(14)	119.8(7)
C(13)-C(14)-C(15)	120.2(5)	C(13)-C(14)-C(15)	119.1(7)
N(3)-C(15)-C(14)	120.8(5)	N(3)-C(15)-C(14)	120.2(7)
F(6B)-P(1)-F(4B)	178(2)	O(3)-Cl(2)-O(2)	111.0(4)
F(6B)-P(1)-F(5B)	81.7(19)	O(3)-Cl(2)-O(4)	107.8(5)
F(4B)-P(1)-F(5B)	96.6(18)	O(2)-Cl(2)-O(4)	109.5(4)
F(6B)-P(1)-F(4A)	131.1(18)	O(3)-Cl(2)-O(1)	110.4(4)
F(4B)-P(1)-F(6A)	133.8(16)	O(2)-Cl(2)-O(1)	110.8(4)
F(5B)-P(1)-F(6A)	129.6(10)	O(4)-Cl(2)-O(1)	107.2(4)
F(4A)-P(1)-F(6A)	177.5(4)		
F(6B)-P(1)-F(1)	90.1(14)		
F(4B)-P(1)-F(1)	89.3(14)		
F(5B)-P(1)-F(1)	88.8(8)		
F(4A)-P(1)-F(1)	91.1(3)		
F(6A)-P(1)-F(1)	91.2(3)		
F(4B)-P(1)-F(5A)	136.1(16)		
F(4A)-P(1)-F(5A)	88.9(4)		
F(6A)-P(1)-F(5A)	90.0(4)		

F(1)-P(1)-F(5A)	91.1(2)
F(6B)-P(1)-F(3A)	139.5(18)
F(5B)-P(1)-F(3A)	138.7(11)
F(4A)-P(1)-F(3A)	89.3(3)
F(6A)-P(1)-F(3A)	91.7(4)
F(1)-P(1)-F(3A)	90.9(2)
F(5A)-P(1)-F(3A)	177.4(3)
F(6B)-P(1)-F(3B)	93(2)
F(4B)-P(1)-F(3B)	88.1(19)
F(5B)-P(1)-F(3B)	169.1(13)
F(4A)-P(1)-F(3B)	134.9(12)
F(1)-P(1)-F(3B)	81.3(10)
F(5A)-P(1)-F(3B)	135.2(12)
F(6B)-P(1)-F(2)	90.1(14)
F(4B)-P(1)-F(2)	90.6(14)
F(5B)-P(1)-F(2)	91.8(8)
F(4A)-P(1)-F(2)	89.3(3)
F(6A)-P(1)-F(2)	88.5(3)
F(1)-P(1)-F(2)	179.3(2)
F(5A)-P(1)-F(2)	89.5(2)
F(3A)-P(1)-F(2)	88.6(2)
F(3B)-P(1)-F(2)	98.0(10)

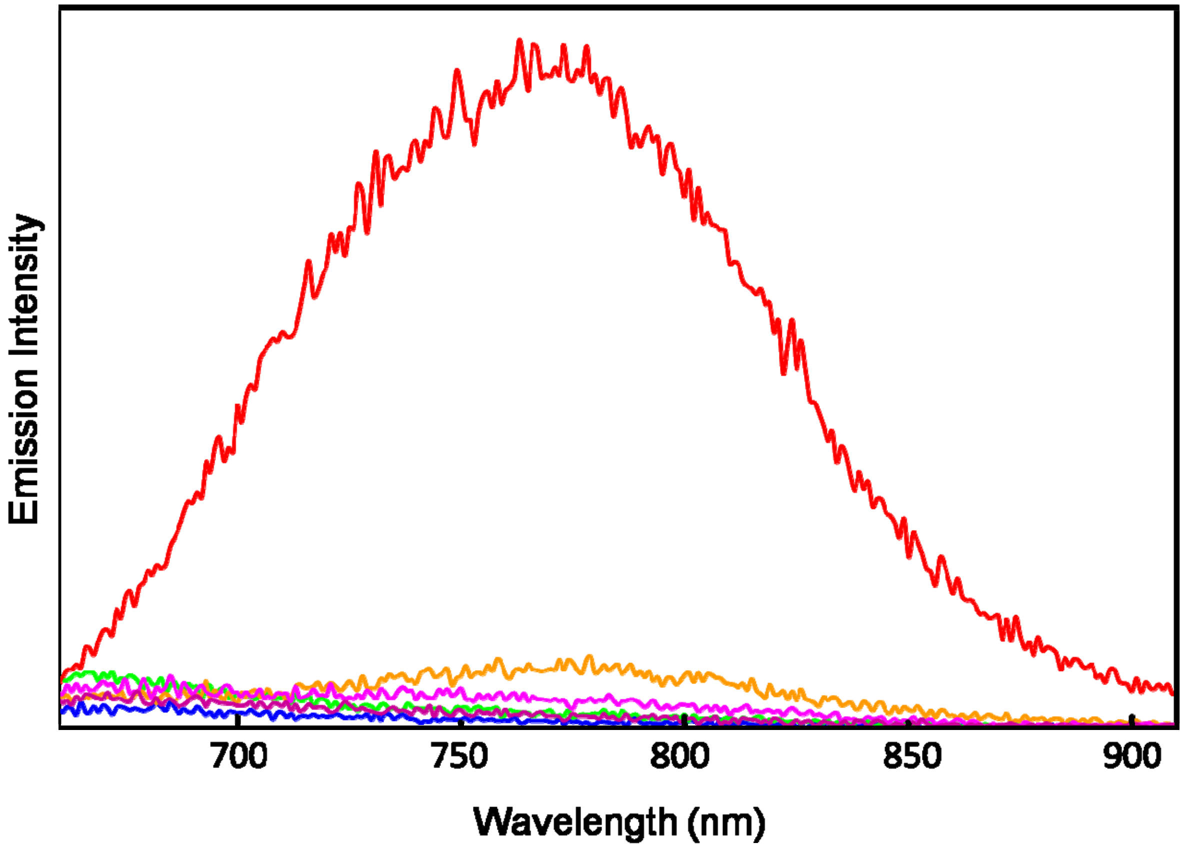

Figure S7 Emission spectra (λ_{ex}=532nm) of **1**•PF_6 supported on Vycor porous glass and immersed in 0.1 M aqueous solutions of water (—), SO_4^{2-} (—), Cl^- (—), CO_3^{2-} (—), NO_3^- (—), and ClO_4^- (—).

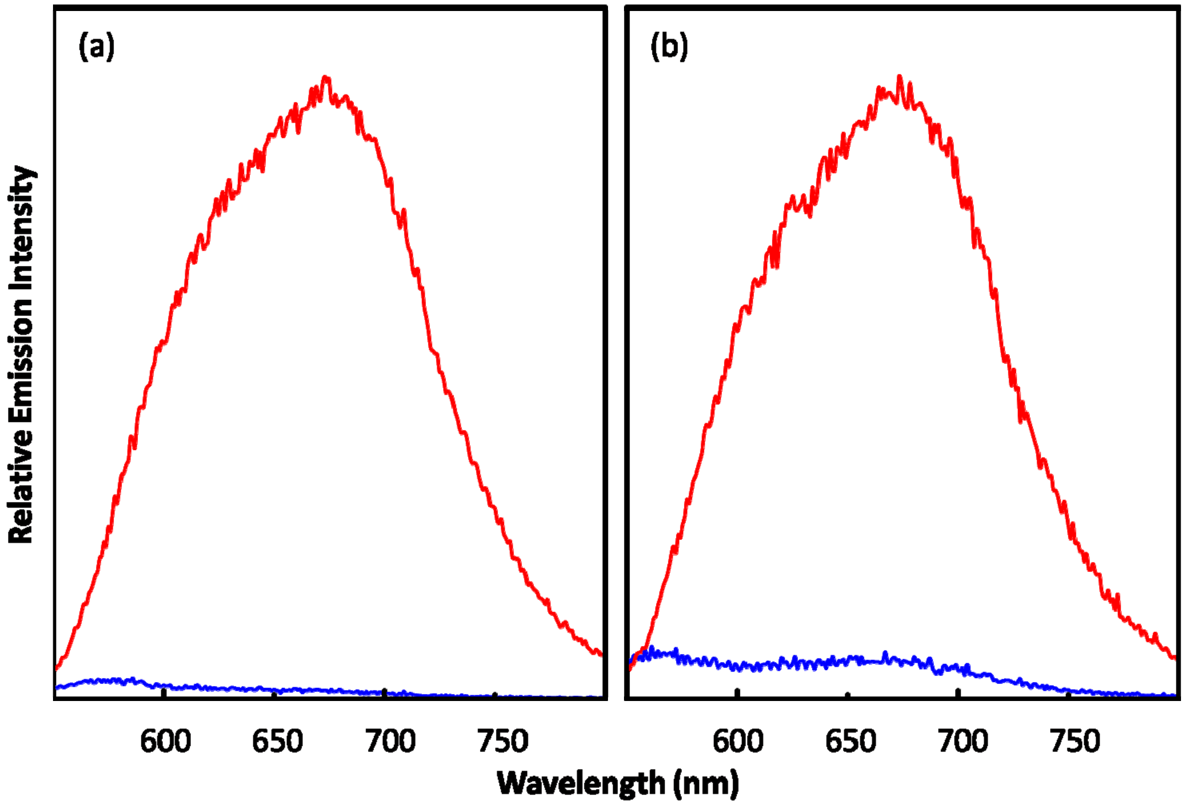

Figure S8 Uncorrected emission spectra (λ_{ex} = 532 nm) of Vycor porous glass supported **1**•PF_6 immersed in (a) homogenized and pasteurized 1% fat Great Value brand milk, and (b) Ohio River water. Spectra were recorded of each solution before (—) and after (—) addition of $NaClO_4$ to give a total ClO_4^- concentration of 0.1 M.

(1) McDermott, J. X.; White, J. F.; Whitesides, G. M. *J. Am. Chem. Soc.* 1976, **98**, 6521-6528.
(2) Annibale, G.; Brandolisio, M.; Pitteri, B. *Polyhedron* 1995, **14**, 451-453.
(3) Bailey, J. A.; Hill, G. M.; Marsh, R. E.; Miskowski, V. M.; Schaefer, W. P.; Gray, H. B. *Inorg. Chem.* 1995, **34**, 4591-4599.
(4) SMART v5.632 and SAINT v6.45A, v7.46A data collection and data processing programs, respectively. Bruker Analytical X-ray Instruments, Inc., Madison, WI; SADABS v2.10, 2008/1 for the application of semi-empirical absorption and beam corrections. G.M. Sheldrick, University of Göttingen, Germany; SHELXTL v6.14 for structure solution, ORTEP figures and tables, neutral-atom scattering factors as stored in this package. G.M. Sheldrick, University of Göttingen, Germany and Bruker Analytical X-ray Instruments, Inc., Madison, WI; DIAMOND v3.2c for packing diagrams. K. Brandenburg, Crystal Impact, Germany.
(5) Dalesio, L. R.; Hill, J. O.; Kraimer, M.; Lewis, S.; Murray, D.; Hunt, S.; Watson, W.; Clausen, M.; Dalesio, J. *Nucl. Instrum. Meth. A* 1994, **352**, 179-184.
(6) Wang, J.; Toby, B. H.; Lee, P. L.; Ribaud, L.; Antao, S. M.; Kurtz, C.; Ramanathan, M.; Von Dreele, R. B.; Beno, M. A. *Rev. Sci. Instrum.* 2008, **79**, 085105.
(7) Lee, P. L.; Shu, D.; Ramanathan, M.; Preissner, C.; Wang, J.; Beno, M. A.; Von Dreele, R. B.; Ribaud, L.; Kurtz, C.; Antao, S. M.; Jiao, X.; Toby, B. H. *J. Synchrotron. Radiat.* 2008, **15**, 427-432.